Al-Mustansiriyah Journal of Science
ISSN: 1814-635X (print), ISSN: 2521-3520 (online)
Volume 29, Issue 3, 2018
DOI: http://doi.org/10.23851/mjs.v29i3.622

Research Article **Open Access**

Zinc Metal Ion Affected the Structural Stability of Amyloid-Like Nanofibrils

Zahraa S. Al-Garawi*
Physical Biochemistry, Chemistry Department, College of Science, Mustansiriyah University, IRAQ.
**email: z.mohsin@uomustansiriyah.edu.iq*

ArticleInfo

Received
07/10/2018

Accepted
21/10/2018

Published
10/03/2019

Abstract

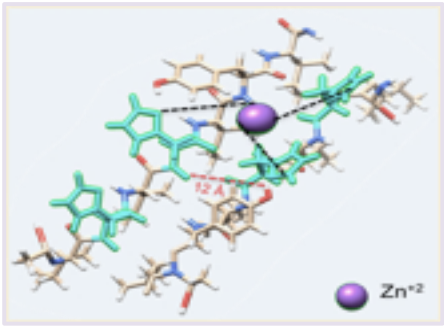

Synthetic peptides that self-assemble into well-defined structures with a cross-β arrangement are called amyloid-like fibrils. Amyloids are associated with a list of disorders and neurodegenerative diseases, such as Alzheimer's and Parkinson`s disease. We previously showed that amyloid-like nanofibrils with a repeating motif "IHIH" were functional fibrils. They were able to bind a metal ion through imidazole moieties and mimic the native carbonic anhydrase enzyme by hydrolysing the CO_2 molecule. Thus, these synthetic amyloid fibrils were suggested to be good candidates to moderate and update the modern enzymatic molecules. This study aims to shed a light on the stability of these amyloid nanofibrils over a study period of 25 days, in the presence/absence of a metal ion. The work continued for approximately 7 months in the Biochemistry department, School of Life Sciences at the University of Sussex in the United Kingdom. A set of designed peptides with a repeating motif "IHIH" were explored, based on some structural studies. Short and long peptides with free ends as well as closed ends were investigated. Peptides allowed to self-assemble with and without a metal ion (zinc) were then examined using circular dichroism, fluorimetry and electron microscopy for structural biophysical analysis. Regardless of the metal ion contribution, peptides showed stable secondary structures with a β-sheet conformation for the incubation time of 25 days. Their morphologies did not appear to change over time. However, the presence of a zinc ion has an effect on the secondary structure of the mature fibrils. Results indicated that fibrils grown with the zinc ion have a significantly higher propensity to form β-sheets secondary structures during incubation time. The presence of a zinc ion also affected the dimensions of the amyloid-like fibrils by the end of the study course, at which point they significantly reduced. This effect of zinc ion on synthetic amyloid fibrils has not been previously reported. The stabilities of the zinc-nanofibrils point to their potential for use in modifying or updating the enzyme-mimic analytical reactions. The effect of adding zinc on the fibrillation seems to be crucial. Although it apparently improved the β-sheet assembly, it affected the width/length of the synthetic amyloids. This effect could be promising toward reducing the generation of amyloid fibrils and ultimately understanding the pathogenesis of Alzheimer disease.

Keywords: Functional fibrils, amyloids, structural stability, circular dichroism.

الخلاصة

البيتيدات الاصطناعية التي لها قابلية التجمع الذاتي وتكوين هياكل ليفية محددة ذات تركيب β الرباعي تسمى بشبيهات ألاميلويد. يرتبط الاميلويد مع قائمة من الاضطرابات والأمراض العصبية، مثل مرض الزهايمر ومرض باركنسون. وضحت دراستنا السابقة أن ألالياف النانوية شبيهة الأميلويد ذات التعاقب المتكرر "IHIH" كانت الياف وظيفية، اذ أظهرت محاكاة ناجحة للانزيم الطبيعي (carbonic anhydrase) عن طريق تآصر مجاميع الاميدازول في الحامض الاميني الهيستدين مع أيون معدني (الخارصين) وتحليل جزيئة p-nitrophenyl acetate التي طالما عمل الانزيم على تحليلها. اقترحت تلك الدراسة ان هذه الالياف الاصطناعية مرشحات جيدة لتطوير نماذج الجزيئات الأنزيمية الحديثة.
تهدف الدراسة الحالية إلى إلقاء الضوء على مدى استقرارية هذه الألياف الاميلويدية النانوية بوجود وعدم وجود ألايون

المعدني، إذ استمر العمل بجمع البيانات مدة ٧ أشهر تقريبا في قسم الكيمياء الحيوية، كلية علوم الحياة في جامعة ساسكس في المملكة المتحدة.

تم استكشاف وفحص مجموعة من الببتيدات المصممة على اساس تكرار التعاقب " "IHIH" بناءً على بعض الدراسات البنيوية سابقة، بعض هذه الببتيدات قصيرة السلسلة (٧ احماض امينية) وأخرى طويلة (١١ حامض اميني) ، وبعضها ذات نهايات لحرة بينما أخرى كانت ذات نهايات مغلقة، كما تم فحص استقرارية جميع الببتيدات بوجود وعدم وجود الخارصين باستخدام عدة تقنيات فيزياحياتية مثل ثنائي اللون الدائري، وجهاز الفلورة، والمجهر إلالكتروني، اذ جمعت البيانات من كل تقنية ثلاث مرات متعاقبة على الأقل وحُلّلت احصائياً.

أظهر معدل النتائج ان لهذه الببتيدات الاصطناعية شكل شبيه الاميلويد مستقر طيلة فترة المتابعة (٢٥ يوماً)، بوجد وعدم وجود الخارصين، ومع ذلك، كان لوجود أيون الخارصين تأثير على البنية الثانوية للألياف الناضجة. أشارت النتائج إلى أن ميل الألياف النامية بوجود أيون الخارصين لتشكيل بنية ثانوية ذات صفائح β يتزايد معنويا بمرور الوقت أكثر من تلك الالياف النامية بعدم وجود الخارصين. ان وجود أيون الخارصين ضمن الياف شبيهات بالأميلويد لفترة طويلة قد أثر على أبعاد هذه الالياف، اذ لوحظ تقلص معنوي في الطول والعرض في نهاية فترة المتابعة، لم تكن مثل هذه التأثيرات قد دُرست وأُدرجت في الادبيات سابقاً.

على اساس ما تقدم، يبدو أن إضافة الخارصين كان له تأثير مهم على التفاف الالياف، فعلى الرغم من تكوين تركيب ثانوي ذو صفائح β بشكل جيد ومُحّسن، كان هناك تأثيراً معنوياً في طول وعرض الالياف الاصطناعية، وهنا، قد يكون هذا التأثير واعداً نحو الحد من توليد الألياف الاميلويدية وفهم مسببات مرض الزهايمر، وبالتالي كيفية علاجه.

Introduction

Zinc is one of the most prevalent transition metal cofactors, which is essential in biological systems. It participates in most hydrolases enzymatic reactions and plays important roles for stabilizing the structure and regulatory functions of thousands of proteins [2, 3]. Compared to other transition metal ion (ions?) , zinc has a filled d-orbital which makes it stable in the biological environment and an ideal cofactor to catalyse a reaction requiring a Lewis acid-model catalyst [4].

According to the hard-soft (acid-base) theory, zinc has a borderline propriety, which enables it to coordinate well with hard donor atoms (such as nitrogen and oxygen) and soft donors (sulphur). It can coordinate to the N_{δ} or N_{ε} atom of the imidazole ring of histidine amino acid residue and coordinate to the $O_{\varepsilon 1}$ or $O_{\varepsilon 2}$ atom of glutamic acid or aspartic acid (syn or anti), as well as the S atom of cysteine amino acid residues [3, 5].

Previous studies reviewed the designing of a proper zinc-binding site as scaffolds toward building up a metalloenzyme for hydrolytic reactions [6]. However, designing zinc metalloenzyme molecule or enzyme-like catalyst is still one of the current challenges. The required number of histidine to create an active site depends on the type of the required catalyst. To coordinate zinc and functionalize the scaffold, usually two histidines at least should be available [7]. Several synthetic peptides which were known to self-assemble into amyloid-like fibrils were attractive models to mimic the esterase hydrolyse activity via the zinc-binding approach [1, 8, 9]. The peptides formed β-sheets where two histidine ligands from one strand bound zinc and bridged with a third histidine from an adjacent strand to form a metal-histidine chain along the fiber axis. The NMR investigation revealed that binding with zinc played an efficient role for stabilizing the structure of artificial catalysts and shaping the catalytic reactivity [10]. Amyloid-like fibrils are artificial peptides that are able to self-assemble into strong and stable three-dimensional architecture, depending on the constituent amino acid side chains. They are created to mimic the native complex amyloid fibrils, for potential applications [11-13]. Amyloid fibrils are characterized by their regular cross-β architecture [14]. They are a misfolded state of native proteins, aggregate within organs and tissues and associated with some disorders and neurodegenerative diseases such as Diabetes type 2, Alzheimer`s, Spongiform encephalopathies and Parkinson’s [15, 16].

Despite this apparent complexity, such self-assemblies possess varied roles in a wide range of applications, including bio-nanotechnology, medicinal, pharmaceutical and material sciences [8, 17-23].

Here, we tried to understand the stability of self-assemblies of four amyloidogenic designs over a specific time frame and temperature, where they bound zinc at the imidazole moieties. Peptides were rationally designed with free and closed ends and with seven and

eleven residues to build-up single and double binding sites by an alternating sequence of isoleucine (I) and histidine (H) at a position *i* and *i+2* to create a motif of "IHIH" for zinc-binding site [1]. These designs were based on a known design [24], but were modified to involve tyrosine (Y) at position 6 to promote the affinity toward binding zinc. Transmission electron microscopy, circular dichroism and fluorimetry were used to monitor the self-assembly and amyloidogencity in the presence of zinc within the fibrils over a long-time frame and to examine how the secondary structure could be affected.

Materials and Methodologies

Materials

Tris-base buffer was purchased from Fisher Scientific, $ZnCl_2$ (Sigma-Aldrich) and TEM copper grids (400 mesh, with Carbon/Formvar film) from Agar Scientific. Quartz cuvettes (1 cm) for foluorimetry was purchased from Starna, Essex, UK. Quartz cuvettes (1mm) for circular dichroism was purchased from Sigma-Aldrich. 0.2 μM filtered milli-Q water was used to prepare solutions for all experiments.

Synthesis of peptides: Peptides in Table 1 were designed and synthesized in an earlier work [1].

Briefly, peptides were synthesized using standard peptide synthesis and cleavage protocol assisted by a microwave solid phase peptide synthesizer (Liberty Blue CEM). Fmoc-protected ChemMatrix® resins (loading of 0.49mmol/g) were used to synthesize the capped peptides (**3** and **4**). The uncapped peptides (**1** and **2**) were synthesized using high swelling, low loading Wang resin (Loading 0.24 mmol/g) [1].

Peptide stock and working solution

Stock peptide solution (1.1 mM) was prepared by adding 10 mM HCl to the crude peptides. To prepare working solutions (with/without Zn^{2+}): 180 μL of the stock solution was mixed with 20 μL of 2-propanol and 1.8 mL Tris-base buffer solution (25 mM, pH 8, with /without 1 mM $ZnCl_2$) as previously described [1, 24]. All peptides were incubated at 37 °C for 25 days.

Transmission electron microscopy (TEM): Four μL of 99μM of working peptide solutions were incubated for two min on the copper grid and then negatively stained using 4 μL of 2% uranyl acetate for two min. Excess liquids were blotted off at each step using a filter paper after each incubation. This experiment was repeated for all peptides over a time course starting at zero-time fibrillation (0t), 3, 17 and continued up to 25 days. Grids were examined using a Hitachi 7100 electron microscope operated at 80 kV and images were collected on a CCD detector. ImageJ 1.50i (Wayne Rasband, National institutes of Health, USA) was used for processing and analyzing the images and measuring fibrils dimensions.

Circular dichroism (CD): Nighty nine μM of working peptide solutions (with/without Zn^{2+}) were examined using circular dichroism spectroplarimetry. The wavelength setting was between 180–320 nm, a pitch of 0.1 nm, a scan speed 50 nm/min, response time 4 s, slit widths 1 nm and with a standard sensitivity. Care was taken to wash the cuvettes before and after use with 2% Hellmanex, water, ethanol, and then air-dried. For clarity, Tris-base buffer reading (with/without Zn^{+2}) was subtracted from peptide readings. Peptide solutions were monitored at different times (0t, 3, 17 and 25 days) and data was collected in triplicates using a Jasco J-715 spectropolarimeter with a temperature control system at 20˚C.

Fluorescence assay

1. Thioflavin T fluorescence assay (ThT)

A stock of 1.5 mM of the dye ThT (in water) was filtered using 0.2 μm filter paper and mixed gently with peptide working solutions (with/without Zn^{+2}) to prepare a solution of 30 μM and then incubated for 3-5 min to enable binding of the dye with the peptide. Blank solutions were similarly treated, but with Tris-base buffers (with/without Zn^{+2}) instead of peptide solutions, to be subtracted from

readings. Data was collected in triplicate; the excitation was at λ-450 nm and intensities collected at ~ λ-485 nm. Excitation and emission slits were set to 5 and 10nm respectively; the scan rate was 600nm/min with 0.1 s as an average time and at 1 nm intervals.

2. *Tyrosine fluorescence emission*:
Fluorescence emission spectra of working peptide solutions (99μM), with/without Zn^{2+}, were collected in triplicate, with an excitation of λ-280 nm and emission of λ-305 nm. The excitation and emission slits were set to 5 nm, scan rate was 600 nm/min with 1nm data intervals and an average time of 0.1 s. Care was taken to wash the cuvettes before and after use with 2% Hellmanex, water, ethanol, and then air-dried.
All the fluorescence data were carried out on a Varian Cary Eclipse fluorimeter (Varian Ltd., Oxford, UK) with a high voltage of photomultiplier (800v) at 20˚C.
Peptides in Table 1 were rationally designed for structurally characterizing and understanding their potential to be functional amyloid-like fibrils [1, 25].

Table 1: Peptide designs.

1	NH_2-Ile-His-Ile-His-Ile-Tyr-Ile-OH
2	NH_2-Ile-His-Ile-His-Ile-Tyr-Ile-His-Ile-His-Ile-OH
3	CH_3CO-Ile-His-Ile-His-Ile-Tyr-Ile-NH_2
4	CH_3CO-Ile-His-Ile-His-Ile-Tyr-Ile-His-Ile-His-Ile-NH_2

(a) IHIHIYI 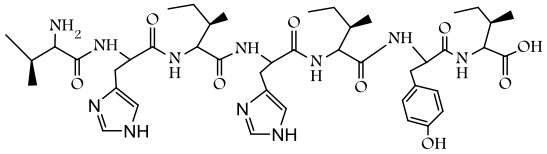

(b) IHIHIYIHIHI 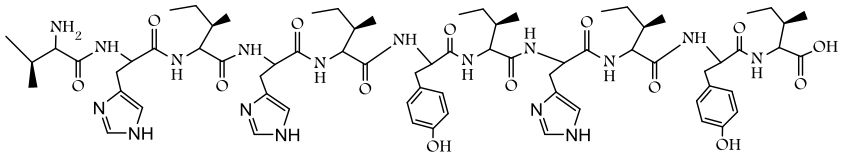

(c) Ac–IHIHIYI–NH_2 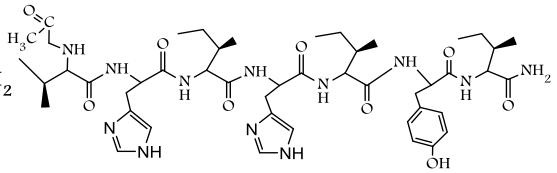

(d) Ac–IHIHIYIHIHI–NH_2 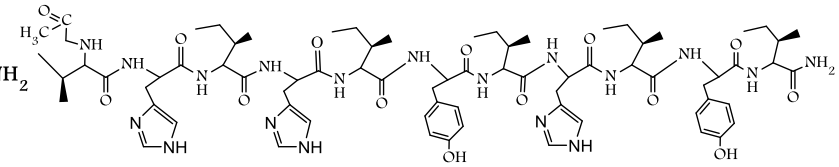

- Amino acid codes: Isoleucine (I), histidine (H), tyrosine (Y) and CH_3CO (Ac).

Figure 1: peptides assembled with zinc-peptides as well as without zinc-free peptides.

Results and Discussion

Self-assembly of designed peptides

Electron microscopy was used to follow the morphologies and the influence of zinc on the self-assembly over the course of 25 days.
Images in Figure 1 show that peptides assembled with zinc (zinc-peptides) as well as peptides assembled without zinc (zinc-free peptides), self-assembled as soon as they were dissolved. The uncapped peptides **1** and **2** were longer than those of capped peptides. Peptide **1** formed wavy nanofibrils at zero-time fibrillation (0t) and elongated over time. Peptide **2** folded into twisted long nanofibrils at 0t, and then laterally associated into stack

Volume 29, Issue 3, 2018 DOI: http://doi.org/10.23851/mjs.v29i3.622

masses. Capped peptides **3** and **4** formed thin nanofibrils with variant sizes. Peptide **3** was a short and straight nanofibrils at 0t, then grew further with different sizes over time. Peptide **4** assembled quickly into twisted short nanofibrils at an early stage and laterally associated over time; see Figure 1 (a-d).

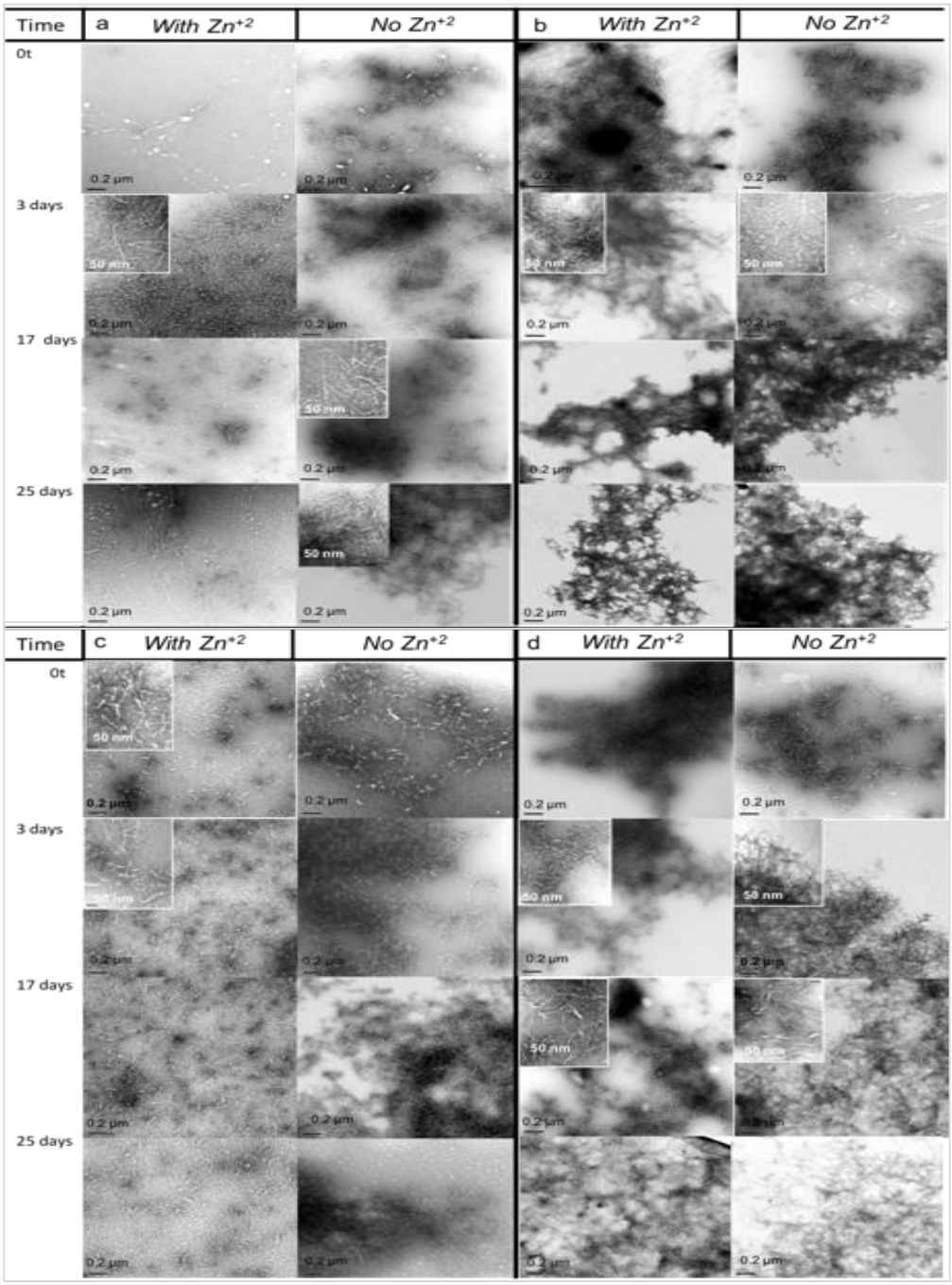

Figure 1: Electron microscopy images of peptides **1**- **4** self-assembled with/without 1mM $ZnCl_2$ in 25mM Tris-base buffer, pH 8. Morphology of peptides followed over 25 days.

***Circular dichroism (CD)* spectroscopy**

This technique is frequently used to investigate the secondary structure content and the

folding/misfolding of proteins (Greenfield 2006, Kelly et al. 2005, Kelly and Price 1997, Kelly and Price 2000). All peptides (with/without Zn^{2+}) folded into a stable β-sheets secondary structure, where minima of ~ λ 218 - 220 nm were observed over the study course. Different elipiticities were observed depending on the type of the peptide and its age. This experiment was repeated for two sets of peptides assembled at two different temperatures (room temperature and 37° C) to study the effect of temperature on the folding process. No significant differences were indicated between the CD spectra at the different temperatures, see Figure 2.

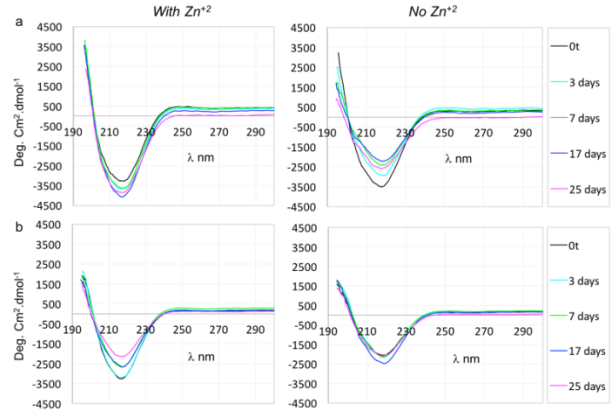

Figure 2: The CD spectra of two examples: peptide **3** and **4** assembled at 37° C in the presence (left) and absence (right) of zinc over 25 days. a) peptide **3** and (b) peptide **4**.

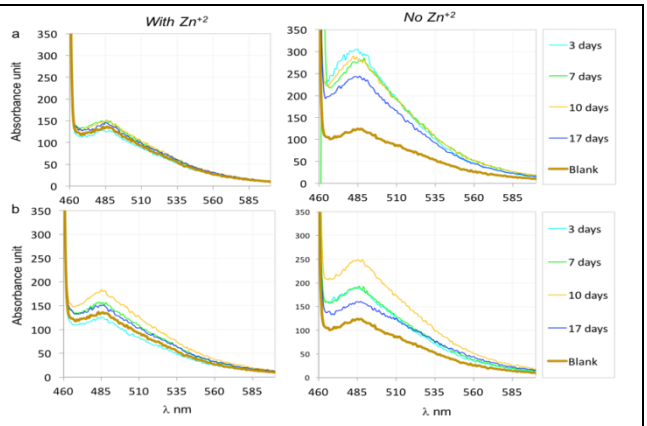

Figure 3: The ThT fluorescence emission of peptide **3** and **4** in the presence (left) and absence (right) of zinc over a study course of 25 days**.** a) peptide **3** and (b) peptide **4**.

Thioflavine T (ThT) fluorescence

This assay is a good indicator for self-assembly into amyloids (Levine 1993). It binds amyloid fibrils through a critical mechanism (Biancalana and Koide 2010). It is therefore used here to examine the self-assembly into amyloid, in the presence/absence of zinc. We recently reported that these peptides bound the dye ThT with fluorescence intensity signals monitored at ~ λmax 480- 483 nm. However, zinc-free peptides showed the highest intensity of ThT signals over time compared to those assembled with zinc (Al-Garawi et al. 2017), see Figure 3.

Tyrosine fluorescence

is often used to follow any change in the tyrosine environment during the self-assembly events (Lakowicz 2007). Spectra of tyrosine fluorescence emission over 25 days are shown in Figure 4 (a-d). Results indicated that tyrosine emitted at different wavelengths depending on the peptide type and age and availability of Zn^{+2}. This experiment was repeated for two sets of peptides assembled at two different temperatures (room temperature and 37° C) to study the effect of temperature on the folding process. Spectra at room temperature were not significantly different compared with these of 37° C.

In the presence of Zn^{+2}, peptides emitted tyrosine at ~ λmax 307-322 nm over the study frame-time. In the absence of Zn^{+2}, peptides have shown little signals at around λmax 310-315 nm within the first 10 days and then shifted to appear at ~ λmax 345-357. Moreover, additional signals observed by the end of the study course were close to ~ λ max 402-417 nm. The shifts in the emission wavelengths and the additional peaks were not detected in zinc- peptides as illustrated in Figure 4 and Table 2.

Table 2: Tyrosine emission wavelengths of peptides (**1-4**) self-assembled with/without Zn^{+2}. Arrows indicate that the emission wavelength at 0t has red-shifted after 25 days.

	Time/ days	**1**	**2**	**3**	**4**

With Zn^{+2}	0t→25	317 – 320 nm	322 nm	345- 347 nm	307– 312 nm
No Zn^{+2}	0t→25 (additional peaks)	310 nm →357nm 407- 410 nm	315nm →357 nm 402-407 nm	347nm→350 nm No shift	312 nm→ 402 nm 405 nm→417 nm

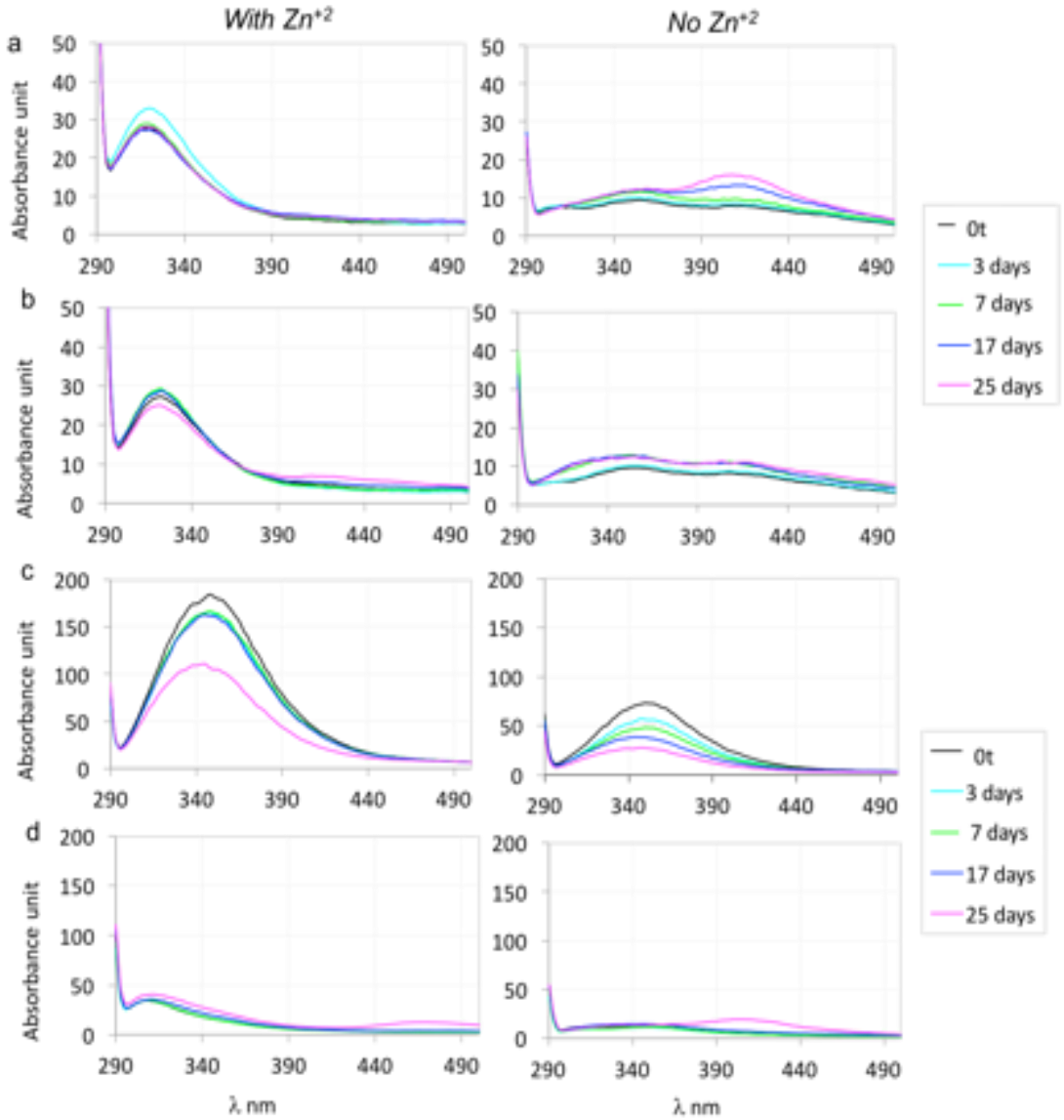

Figure 4: The tyrosine fluorescence emission of peptides **1**- **4** in the presence (left) and absence (right) of zinc over 25 days**.** a) peptide **1**, b) peptide **2**, c) peptide **3** (permitted by [1] and d) peptide **4**.

The structural stability of amyloid nanofibrils in the presence of zinc

Peptide dimensions: Although Zn^{2+} did not show an influence on the peptide morphologies, it affected the fibril dimensions by the end of the study course. At 0t fibrillation, short and twisted nanofibrils of **1** and **2** were observed**.** By the end of the course, peptides assembled with zinc demonstrated narrower nanofibrils than peptides free of zinc (3.3-12.6 nm *vs* 4.2-14 nm, respectively) and with different lengths. Nanofibrils of peptides **3** and **4** were significantly shorter ($p<0.02$ and $p<0.0004$, respectively) and narrower in the presence of zinc by the end of the experiment ($p<0.0001$ and $p<0.04$ respectively), see Figure 1 and Figure 5a.

The secondary structure: The self-assembly with zinc did significantly help to improve the CD signals of β-sheets content more than that of zinc-free peptides ($0.0007<p<0.025$). However, this change wasn't significant for uncapped peptides (**1** and **2**, $p>0.05$), Figure 5b.

ThT binding: Peptides free of zinc have intense ThT-binding signals over those of zinc-peptides, specifically, peptides **3** and **4** ($0.01<p<0.05$), Figure 5c.

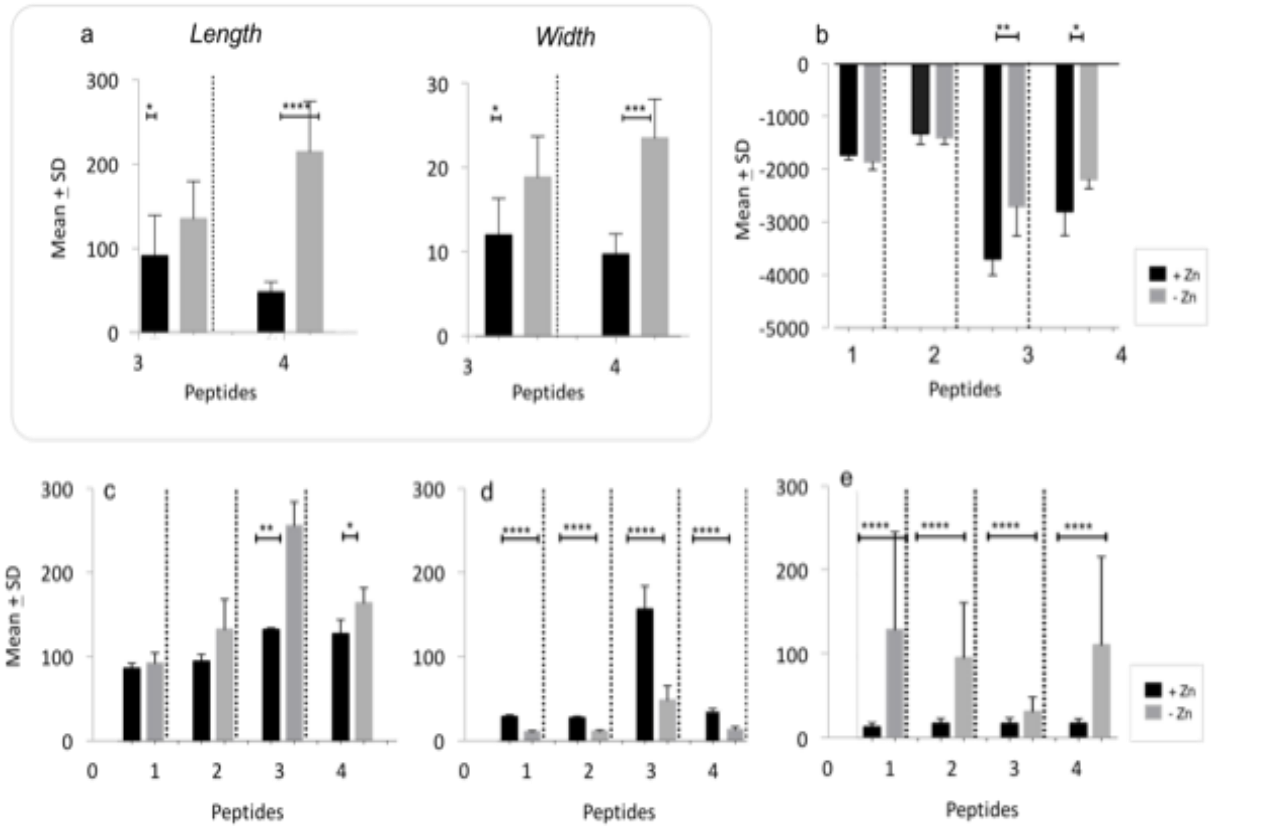

Figure 5: Statistical analysis of the effect of zinc on the dimensions and structure of peptides under study. a) Dimensions of the capped peptides after 25 days fibrillation in tris pH 8. b) Effect of zinc on β-sheet intensity over 25 days fibrillation in Tris-base, pH 8 at 37 °C. Each bar represents 5 independent runs at different time points (0t, 3, 17, and 25 days). c) ThT- binding emissions over 25 days. d) Tyrosine fluorescence up to 25 days fibrillation at 37 °C and e) Di-tyrosine emissions after 25 days. the Each bar in (c), and (e Average of 5 independent runs at different time points. RISIM version 7 GraphPad software was used to find the analysis using the unpaired t-test and two tail p values considered significant only if $p<0.05$, shows as stars over scale bars.

Discussion

Designing short peptides to self-assemble into functional amyloid-like fibrils has been previously reported [26, 27]. We previously showed that different self-assemblies formed functional amyloid-like fibrils depending on the sequence and the type of side chains. They were good templates to form chemically and thermally stable silica nanowires [23, 28] and were the provided scaffolding for a diverse range of applications [12]. We also developed some amyloidogenic designs with an active site to understand their structure and the potential to act as a hydrolase enzyme-like catalyst [1] based on a previous study [24]. This study aims to study in-depth the effect of adding zinc on the stability of these functional amyloid-like nanofibrils over time.

Design strategies for the hydrolytic peptides have been described previously [1]. Briefly, 7mer peptides (**1** and **3**) were designed as model peptides with a single binding site, to

study the structure, zinc-binding and the hydrolysis activity compared to 11mer peptides (**2** and **4**). The incorporation of alternative polar isoleucine and charged histidine was expected to enhance the self-assembly [29]. Histidine residues are known to support zinc-binding through the imidazole moieties [6, 24, 30].

All Peptides in Table 1 self-assembled into amyloid-like fibrils with a cross-β arrangement [1]. Electron microscopy images showed extensive nano-fibrils from the first day of fibrillation until the end of the study course. Interestingly, although we previously showed by X-ray fiber diffraction that zinc did not affect the whole architecture of the peptides, analysing the electron microscopy images in Figure 1 revealed slight changes in the dimensions. Zinc-peptides produced relatively shorter and narrower nanofibers than those free of zinc, see Figure 1, and Figure 5a. This could be explained by the effect of Zn^{2+} to reduce lateral associations. Zinc was previously suggested as a key role in the generation of amyloid fibrils [31]. It has been predicted to bind the N-terminus of amyloid-β and fold the N-terminus around the zinc, which formed shorter species. It thus interfered with the kinetics of aggregation process of amyloid-β fibrils [32].

The CD spectra are used for monitoring any change in the secondary structure of peptides when there is a change in temperature, pH and concentration [33]. Peptides with and without zinc showed a good evidence of β-sheet contents over the study course. Figure 2 shows two examples for peptides **3** and **4**. This might be interpreted to the support effect of tyrosine at position 6. Furthermore, data indicated significant larger ellipticity values of β-sheets contents for peptides **3** and **4** which assembled with zinc ($0.0007<p<0.028$), Figure 5b. This is perhaps due to the fact that shorter fibrils are more visible to the CD light, therefore more β-sheet is observed. Alternatively, it could be due to a synergistic effect of Zn^{+2} with the pH of the experiment, which promotes β-sheets formation. It could also be explained by the effect of Zn^{+2} in lowering the net charges of peptides, which possibly enhanced the lateral association of β-sheet. Assuming that, we would expect that amyloid fibrils could be stabilized by adding Zn^{+2}.

However, zinc-peptides showed lower ThT emission spectra than zinc-free peptides ($p<0.05$), Fig 5c. The ThT dye has been well known as a method to follow amyloidogenesis. It is possible that zinc bound the aminobenzole ring of ThT and quenched the signal. This reduction of ThT signal is frequently observed in amyloidogenic peptides when some peptides precipitate out of the solution [34].

The naturally occurring fluorophores tyrosine, phenylalanine, and tryptophan are used for studying any change in peptides conformation. Tyrosine emission provides information on whether the residue is buried inside the fiber structure. However, the intensity of the fluorescence variation depends on the environment (pH of the buffer, temperature, peptide concentration) [34, 35].

Figure 4 showed tyrosine fluorescence emission for all peptides. Zinc-free peptides have significant lower emission intensities than peptides with zinc ($p<0.0001$) with red-shift signals to ~ 347-357 nm, see also Table 2 and Figure 5d. Tyrosine emission is sensitive to the pH; in the ground state *p*Ka of OH^- is near 10 and at high pH the phenolic OH is ionized. In the presence of a basic group such as imidazole, which interacts with the excited state, tyrosine undergoes an excited state ionization and *p*Ka of OH^- will be reduced to 4. As a result, the hydroxyl group might dissociate during the lifetime of the excitation, which leads to tyrosine quenching and forming tyrosinate. Tyrosinate causes a red-shift emission at λ_{max} 345-350 nm [35-37]. Therefore, peptides with more imidazole site chains will decrease the emission intensity, and shift tyrosine fluorescence. Incorporating of Zn^{+2} has its effect on the protonated histidines at pH 8. The interaction with the neighbour phenolic OH^- in the exited state is reduced, without tyrosine quenching, and therefore larger intensities are observed.

On the other hand, zinc-free peptides showed intense fluorescence spectra close to λ_{max} 402-417 [1], which were related to di-tyrosine cross-links [38, 39]. No similar signals recorded by zinc-peptides, where coordination of zinc with histidines from two strands is in the same plane as the tyrosines which may prevent the cross linking. Tyrosinate formation and di-tyrosine cross-links, could explain the early disappearance of tyrosine at λ_{max} 307 nm in peptides free of zinc. Di-tyrosine cross links can stabilize the amyloid structures. Figure 6e indicates significant di-tyrosine formation when zinc was absent, ($p<0.0001$).

According to our previous X-ray fiber diffraction data, two possible models of zinc binding sites have been suggested, where peptides were arranged into two parallel β-sheets [1]. The peptides in these models were oriented either parallel or antiparallel across the β-sheets. Thus, there could be two possible paths for zinc to coordinate with histidines in the parallel arrangement and another two possibilities for the antiparallel arrangement of the 7mer peptides, see Scheme 1a and b.

Peptides with double active centers (**2** and **4**) may have four possibilities for antiparallel and four possibilities for parallel orientations, although no previous models have been reported for this peptide. Scheme 1c demonstrates the possible interactions with only one orientation.

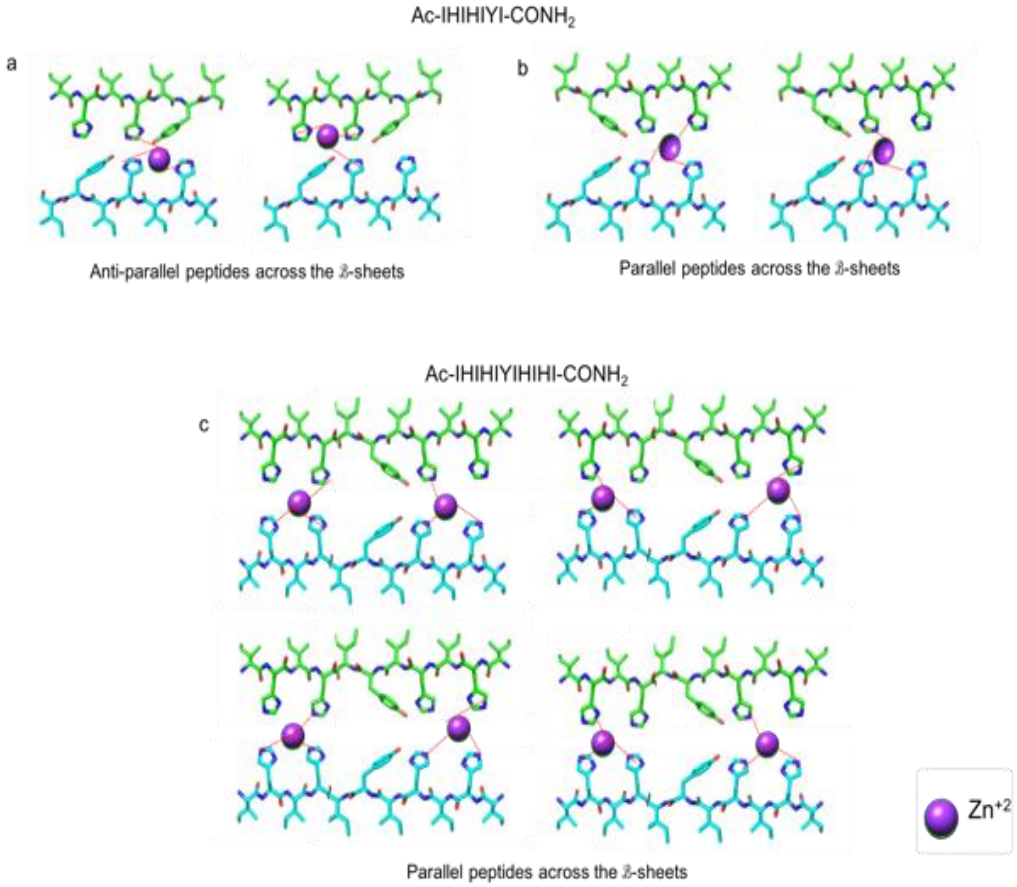

Scheme 1: The possible interactions between zinc and histidines in peptide **3** (top) and **4** (bottom). Zinc coordinates 2 histidines from one strand and another histidine from another strand. a) the possible interaction of zinc with the anti-parallel and b) with parallel orientations of peptide **3**, c) zinc coordination with the parallel orientation of peptide **4.**

Conclusions

This study proposed to explore the effect of zinc on the stability of amyloid-like nanofibrils and their structures over time. Results of TEM, CD and ThT suggest that all peptides were structurally stable over 25 days. However, adding zinc could have an effect on the folding

propensity of some peptides. The effect was mainly shown for peptides with capped ends, where zinc promoted the folding into β-sheets conformation. Zinc also displays a significant effect on the dimensions of the capped peptides over time. Fibrils assembled with zinc were shorter and narrower fibrils after 25 days. Zinc interfered with the fluorescence emission of ThT and tyrosine, compared with zinc-free peptides. It showed lower ThT emission, maybe due to ThT quenched by zinc. Zinc could accelerate peptides aggregation, therefore showing higher tyrosine emission compared with peptides free of zinc. It also prevented di-tyrosine links which were significantly observed without zinc. Our data reveal that zinc affected the dimensions, the folding and the fluorescence emissions of ThT and tyrosine. The interference of zinc with uncapped peptides seemed to be non-significant. Results may have an impact to understanding the degeneration of the amyloid-β fibrils, which is associated with the neurodegenerative Alzheimer disease.

Acknowledgment

This research was supported by a grant to Zahraa S. Al-Garawi from the Iraqi Ministry of Higher education and scientific research, facilitated by Iraqi Cultural Attaché in London. We are thankful to Bennett McIntosh (Preston University- Colorado, USA) for useful discussions.

References

[1] Al-Garawi, Z. S., McIntosh, B. A., Neill-Hall, D., Hatimy, A. A., Sweet, S. M., Bagley, M. C. & Serpell, L. C. (2017) The amyloid architecture provides a scaffold for enzyme-like catalysts, *Nanoscale.* **9**, 10773-10783.

[2] Andreini, C., Lucia Banci, L., Ivano Bertini, I. & Rosato, A. (2006) Counting the Zinc-Proteins Encoded in the Human Genome, *J Proteome Research.* **5**, 196-201.

[3] Sousa, S. F., Lopes, A. B., Fernandes, P. A. & Ramos, M. J. (2009) The zinc proteome: A tale of stability and functionality., *Dalton Trans*, 7946–7956.

[4] Butler, A. (1998) Acquisition and utilization of transitionmetal ions by Marine organisms in *Chemistry and Biology of the oceans* pp. 207-210, Scince,

[5] Auld, D. S. (2001) Zinc coordination sphere in biochemical zinc sites., *BioMetals.* **14**, 271-313.

[6] Zastrow, M. L. & Pecoraro, V. L. (2014) Designing hydrolytic zinc metalloenzymes, *Biochemistry.* **53**, 957-978.

[7] McCall, K. A., Huang, C.-c. & Fierke, C. A. (2000) Function and mechanism of zinc metalloenzymes. in *Zinc and health: Current status and future directions* pp. 1437S-1446S, Amer Soc Nutrit Sci,

[8] Guler, M. O. & Stupp, S. I. (2007) A Self-assembled nanofiber catalyst for ester hydrolysis, *J Am Chem Soc.* **129**, 12082-12083.

[9] Rufo, C. M., Moroz, Y. S., Moroz, O. V., ʾhr, J. S., Smith, T. A., Hu, X., DeGrado, W. F. & Korendovych, I. V. (2014) Short peptides self-assemble to produce catalytic amyloids, *Nature Chemistry, Advance online pubilication*, 1-7.

[10] Lee, M., Wang, T., Makhlynets, O. V., Wu, Y., Polizzi, N. F., Wu, H., Gosavi, P. M., Stohr, J., Korendovych, I. V., DeGrado, W. F. & Hong, M. (2017) Zinc-binding structure of a catalytic amyloid from solid-state NMR, *Proceedings of the National Academy of Sciences of the United States of America.* **114**, 6191-6196.

[11] Morris, K. L., Rodger, A., Hicks, M. R., Debulpaep, M., Schymkowitz, J., Rousseau, F. & Serpell, L. C. (2013) Exploring the sequence-structure relationship for amyloid peptides, *The Biochemical journal.* **450**, 275-83.

[12] Al-Garawi, Z. S., Morris, K. L., Marshall, K. E., Eichler, J. & Serpell, L. C. (2017) The diversity and utility of amyloid fibrils formed by short amyloidogenic peptides, *Interface Focus.* **7**, 20170027.

[13] Kim, S., Kim, J. H., Lee, J. S. & Park, C. B. (2015) Beta-Sheet-Forming, self-assembled peptide nanomaterials towards optical, energy, and healthcare applications, *Small J.* **11**, 3623-3640.

[14] Morris, K. L. & Serpell, L. C. (2012) X-ray fibre diffraction studies of amyloid fibrils, *Methods in molecular biology.* **849**, 121-135.

[15] Knowles, T. P., Vendruscolo, M. & Dobson, C. M. (2014) The amyloid state and its association with protein misfolding diseases, *Nature reviews Molecular cell biology.* **15**, 384-96.

[16] Pawar, A. P., Dubay, K. F., Zurdo, J., Chiti, F., Vendruscolo, M. & Dobson, C. M. (2005) Prediction of "aggregation-prone" and "aggregation-susceptible" regions in proteins associated with neurodegenerative diseases, *Journal of molecular biology.* **350**, 379-92.

[17] Ryan, D. M. & Nilsson, B. L. (2012) Self-assembled amino acids and dipeptides as noncovalent hydrogels for tissue engineering, *Polym Chem.* **3**, 18-33.

[18] Lakshmanan, A., Zhang, S. & Hauser, C. A. (2012) Short self-assembling peptides as building blocks for modern nanodevices, *Trends in biotechnology.* **30**, 155-65.

[19] Dehsorkhi, A. & Hamley, I. W. (2014) Silica templating of a self-assembling peptide amphiphile that forms nanotapes, *Soft matter.* **10**, 1660-1664.

[20] Rajagopal, K. & Schneider, J. P. (2004) Self-assembling peptides and proteins for nanotechnological applications, *Current opinion in structural biology.* **14**, 480-486.

[21] Cherny, I. & Gazit, E. (2008) Amyloids: not only pathological agents but also ordered nanomaterials, *Angew Chem Int Ed Engl.* **47**, 4062-9.

[22] Pilkington, S. M., Roberts, S. J., Meade, S. J. & Gerrard, J. A. (2010) Amyloid fibrils as a nanoscaffold for enzyme immobilization, *Biotechnol Prog.* **26**, 93-100.

[23] Al-Garawi, Z. S., Thorpe, J. R. & Serpell, L. C. (2015) Silica nanowires templated by amyloid-like fibrils, *Angew Chem, Int Ed Engl.* **54**, 13327-13331.

[24] Rufo, C. M., Moroz, Y. S., Moroz, O. V., Stohr, J., Smith, T. A., Hu, X., DeGrado, W. F. & Korendovych, I. V. (2014) Short peptides self-assemble to produce catalytic amyloids, *Nature chemistry.* **6**, 303-309.

[25] Al-Garawi, Z. S. (2017) *Biophysical-Biochemical structural basis of self-assemble peptides, for bionanotechnological applications*, University of Sussex, United Kingdom.

[26] Knowles, T. P. & Mezzenga, R. (2016) Amyloid fibrils as building blocks for natural and artificial functional materials., *Adv Mater.* **28**, 6546-6561.

[27] Makhlynets, O. V., Gosavi, P. M. & Korendovych, I. V. (2016) Short self-assembling peptides are able to bind to copper and activate oxygen., *Angew Chem Int Ed.* **55**, 9017-9020.

[28] Al-Garawi, Z. S., Kostakis, G. E. & Serpell, L. C. (2016) Chemically and thermally stable silica nanowires with a β-sheet peptide core for bionanotechnology., *J Nanobiotechnology.* 14, 79-87.

[29] West, M. W., Wang, W., Patterson, J., Mancias, J. D., Beasley, J. R. & Hecht, M. H. (1999) De novo amyloid proteins from designed combinatorial libraries., Proc Natl Acad Sci USA. 96, 11211-11216.

[30] Srivastava, K. R. & Durani, S. (2014) Design of a zinc-finger hydrolase with a synthetic alphabetabeta protein, PloS one. 9, 1-8.

[31] Maynard, C. J., Bush, A. I., Masters, C. L., Cappai, R. & Li, Q.-X. (2005) Metals and amyloid-β in Alzheimer's disease., Int J Exp Path 86, 147–159.

[32] Abelein, A., Gräslund, A. & Danielsson, J. (2015) Zinc as chaperone-mimicking agent for retardation of amyloid β peptide fibril formation., PNAS. 112, 5407–5412.
[33] Fasman, G. D. (1996) Determination of protien secondary structure. in Circular dichroism and the conformational analysis of biomolecules (Venyaminov, S. Y. & Yang, J. T., eds) pp. 69-107, Plenum Press, New York.
[34] Marshall, K. E. (2010) Structural polymorphism of amyloidogenic peptides., Univeristy of Sussex, School of Life Sciences.
[35] Munishkina, L. A. & Fink, A. L. (2007) Fluorescence as a method to reveal structures and membrane-interactions of amyloidogenic proteins., Biochim Biophys Acta. 1768, 1862-85.
[36] Guzow, K., Ganzynkowicz, R., Rzeska, A., Mrozek, J., Szabelski, M., Karolczak, J., Liwo, A. & Wiczk, W. (2004) Photophysical properties of Tyrosine and Its simple derivatives studied by time-resolved fluorescence spectroscopy, global analysis, and teoretical calculations., J Phys Chem B. 108, 3879-3889.
[37] Lakowicz, J. R. (2007) Protien fluorescence spectroscopy in Principles of fluorescence spectroscopy pp. 534-536, Springer, New Yourk, USA.
[38] Sitkiewicz, E., Oledzki, J., Poznanski, J. & Dadlez, M. (2014) Di-tyrosine cross-link decreases the collisional cross-section of abeta peptide dimers and trimers in the gas phase: An ion mobility study., PloS one. 9, e100200.
[39] van-Maarschalkerweerd, A., Pedersen, M. N., Peterson, H., Nilsson, M., Nguyen, T. T. T., Skamris, T., Rand, K., Vetri, V., Langkilde, A. E. & Vestergaard, B. (2015) Formation of covalent di-tyrosine dimers in recombinant α-synuclein, Intrins Disord Prot. 3, 1-12.